Simulation of CO Oxidation in the Presence of Cyclic Gold Thiolate Complexes: The Effect of a Ligand

N. A. Nikitina[a], *, D. A. Pichugina[a], and N. E. Kuz'menko[a]

[a]*Moscow State University, Moscow, 119991 Russia*

*e-mail: nnikitina1719@gmail.com

Abstract—The interaction of CO and O_2 and the subsequent oxidation of CO in the presence of cyclic thiolate and dithiolate complexes of Au(I), which represent the model fragments of gold clusters stabilized with thiolate ligands, were studied using the PBE density functional theory method. On the basis of the calculated values, it was shown that O_2 and CO were weakly bound to a cyclic thiolate complex of Au(I). In the presence of a dithiolate complex, the activation of O_2 and CO and the subsequent oxidation of CO occurred with low activation energies. The results obtained demonstrate the important role of ligands in the catalytic process.

INTRODUCTION

Gold nanoparticles are well-known catalysts for many industrially important oxidation and hydrogenation reactions [1, 2], among which the low-temperature catalytic oxidation of CO serves as a model reaction frequently used for testing new series of catalysts. Gold clusters stabilized by various ligands (phosphine- and phenylacetylene-containing and thiolate ones) are fundamentally new catalytic systems [3–5]. The thiolate cluster $Au_{25}(SR)_{18}$ was obtained and its structure was theoretically predicted by the density functional method [6]; more recently, the structure was confirmed by X-ray diffraction analysis [7]. This cluster contains a core and a shell. The core consists of gold atoms, and the shell contains not only a ligand but also gold atoms that form fastening or cyclic fragments $-SR-(Au-SR-Au)_x-$ of different lengths.

The synthesized series of gold clusters stabilized by thiolate ligands [8–12] have been actively tested in various applications including catalysis. In particular, their catalytic activity in the oxidation of CO and hydrocarbons and in cross-coupling and hydrogenation reactions was found [13–15]. The undoubted advantage of these catalytic systems is the formation of metal clusters of a certain composition on the surface of a heterogeneous catalyst, which makes it possible to correlate a specific property (activity, selectivity, and stability) with a certain particle size and structure. Liu

et al. [16] carried out such studies and compared the activity of $Au_n(SR)_m$ clusters supported onto hydroxyapatite in the oxidation of styrene.

The promising use of gold clusters stabilized with thiolate ligands in catalysis is hampered by the difficulty of their production in solution because the selectivity of the synthesis is extremely sensitive to reaction conditions. Moreover, the clusters are unstable in solution. Thus, it is well known that a characteristic peak in the UV spectrum of a particular cluster in solution disappeared in one or two days after its preparation [17]. In this case, signals corresponding to the fastening fragments and $(Au(I)-SR)_x$ polymer complexes appeared in the spectrum [17, 18] to indicate the complete or partial destruction of the cluster. This fact suggests the formation of the $(Au(I)-SR)_x$ complexes with the use of $Au_n(SR)_m$ as both homogeneous catalysts and catalysts supported onto the surface of a substrate. At present, the role of fastening fragments in catalytic processes with the participation of gold clusters stabilized by thiolate ligands and the properties of the $Au_n(SR)_m$ cluster remain unclear [19–22].

Here, we report the results of quantum-chemical modeling of the interaction of cyclic Au(I) thiolate and dithiolate clusters with O_2 and CO and the subsequent oxidation of CO in order to establish the catalytic properties of the polymer complexes $(Au(I)-SR)_x$.

Abbreviations: TS, transition state; HOMO, highest occupied molecular orbital; IC, intermediate complex (intermediate).
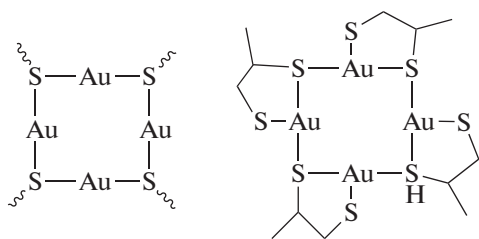
Formulas of the cyclic gold
thiolate and dithiolate complexes

Dithiolate complexes are used along with thiolate complexes for the stabilization of $Au_n(SR)_m$ clusters. The $(AuSR)_4$ cyclic complexes considered in this work are analogs of the previously synthesized compounds $Au_4[SC(Si(CH_3)_3)_3]_4$ [23].

CALCULATION PROCEDURE

The quantum-chemical calculations were performed using the density functional theory with the Perdew−Burke−Ernzerhof (PBE) functional [24] and the SBKJC pseudopotential basis set [25]. Previously, we used this method to determine the structure of $Au_{18}(SR)_{15}$ [26] and to simulate catalytic and adsorption processes with the participation of gold complexes and clusters [27−30].

The equilibrium geometries and total energies were calculated for the test cyclic complexes, the products of their interaction with O_2 and CO, and possible intermediate complexes of CO oxidation. A methyl group was considered as the organic fragment R in the thiolate ligand SR. The contribution of zero-point energies was determined based on the vibration frequencies calculated in a harmonic approximation. Thermodynamic characteristics, including changes in total energy (ΔE) and standard Gibbs energy (ΔG^0) at 298 K, were obtained for all reaction steps. For the most important steps of CO oxidation, the transition

state (TS) structures were localized using the Berny optimization algorithm [31] and the activation energies (E_a) were calculated. The TSs were determined by studying the energy of a reaction system as a function of reaction coordinate using the IRC method [32].

All of the calculations were carried out with the PRIRODA program [33] using the Lomonosov supercomputer at the Moscow State University [34].

RESULTS AND DISCUSSION

At the first stage, the structure of the cyclic Au(I) thiolate complex and its reactivity toward O_2 and CO were studied. Figure 1 shows the optimized structure of $(AuSCH_3)_4$. The $(AuS−)_4$ fragment in the complex is almost planar. An analysis of the type of the highest occupied molecular orbitals (HOMOs) showed that the Au−S bond is covalent. Due to a considerable strength of the Au−S bond in $(AuSCH_3)_4$, CO is not attached and the stable carbonyl complex $(AuSCH_3)_4CO$ is not formed.

The compound $(AuSCH_3)_4O_2$ in a singlet electronic state was obtained as a possible product of the interaction of the cyclic complex with oxygen. Its formation from triplet oxygen is not favorable. Changes in the total energy and the Gibbs energy upon the formation of $(AuSCH_3)_4O_2$ from singlet oxygen, which can be formed on photoactivation in the presence of gold thiolate clusters [35, 36], are insignificant (Table 1). In $(AuSCH_3)_4O_2$, oxygen is weakly activated, as indicated by the O−O distance, which changed only slightly as compared with that in an isolated O_2 molecule (1.22 Å), and the O−O vibrational frequency (1225.3 cm^{-1} compared to 1542.7 cm^{-1} in O_2).

Thus, according to the calculation data, $(AuSCH_3)_4$ does not react with CO, and it is likely that the weak activation of O_2, which requires additional con-
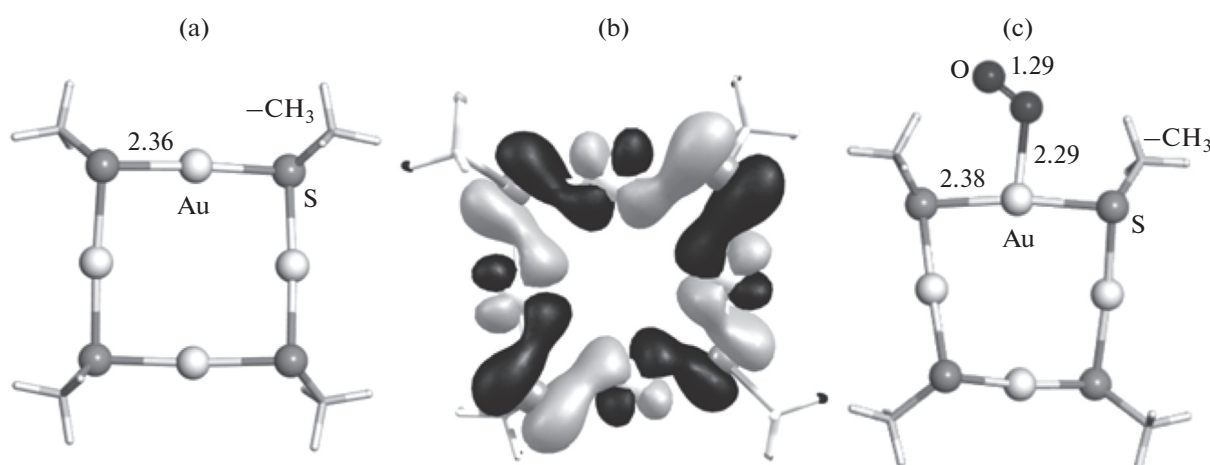
(a) (b) (c)

Fig. 1. Optimized structures of the complexes (a) $(AuSCH_3)_4$ and (c) $(AuSCH_3)_4O_2$ and (b) visualization of the HOMO of $(AuSCH_3)_4$. Key interatomic distances are given in angstrom units.

Table 1. Thermodynamic parameters of the interaction of the cyclic complexes $(AuSCH_3)_4$ and $(AuSCH_2CHSCH_3)_4$ with CO and O_2

| Step	ΔE	ΔG_{298}
	kcal/mol	
$(AuSCH_3)_4 + {}^1O_2 \rightarrow (AuSCH_3)_4O_2$	−12.7	−1.8
$(AuSCH_2CHSCH_3)_4 + {}^3O_2 \rightarrow (AuSCH_2CHSCH_3)_4O_2$	−9.1	−1.3
$(AuSCH_2CHSCH_3)_4 + CO \rightarrow (AuSCH_2CHSCH_3)_4CO$	−9.4	−2.0
$(AuSCH_2CHSCH_3)_4O_2 + CO \rightarrow (AuSCH_2CHSCH_3)_4O_2CO$	−10.3	−3.6

ditions, is insufficient for any further processes involving oxygen.

Next, we investigated the structure of the cyclic Au(I) dithiolate complex and its reactivity toward O_2 and CO. Figure 2 shows the optimized structure of $(AuSCH_2CHSCH_3)_4$. Table 1 summarizes the calculated changes in the total energy and the standard Gibbs energy.

The replacement of a thiolate ligand by dithiolate significantly changed the structure of $(AuSR)_4$. The complex became no planar, and the Au−S distance increased by 0.08 Å. The electron density distribution along the Au−S bond was also different (Fig. 2b). The HOMO was localized on Au and S atoms rather than at the Au−S bond as in the case of $(AuSCH_3)_4$. This fact indirectly indicates an increase in the reactivity of $(AuSCH_2CHSCH_3)_4$. Indeed, the structure of the stable carbonyl complex $(AuSCH_2CHSCH_3)_4CO$ was found, in which the CO fragment is coordinated to two Au atoms. The energy change upon its formation is −9.4 kcal/mol.
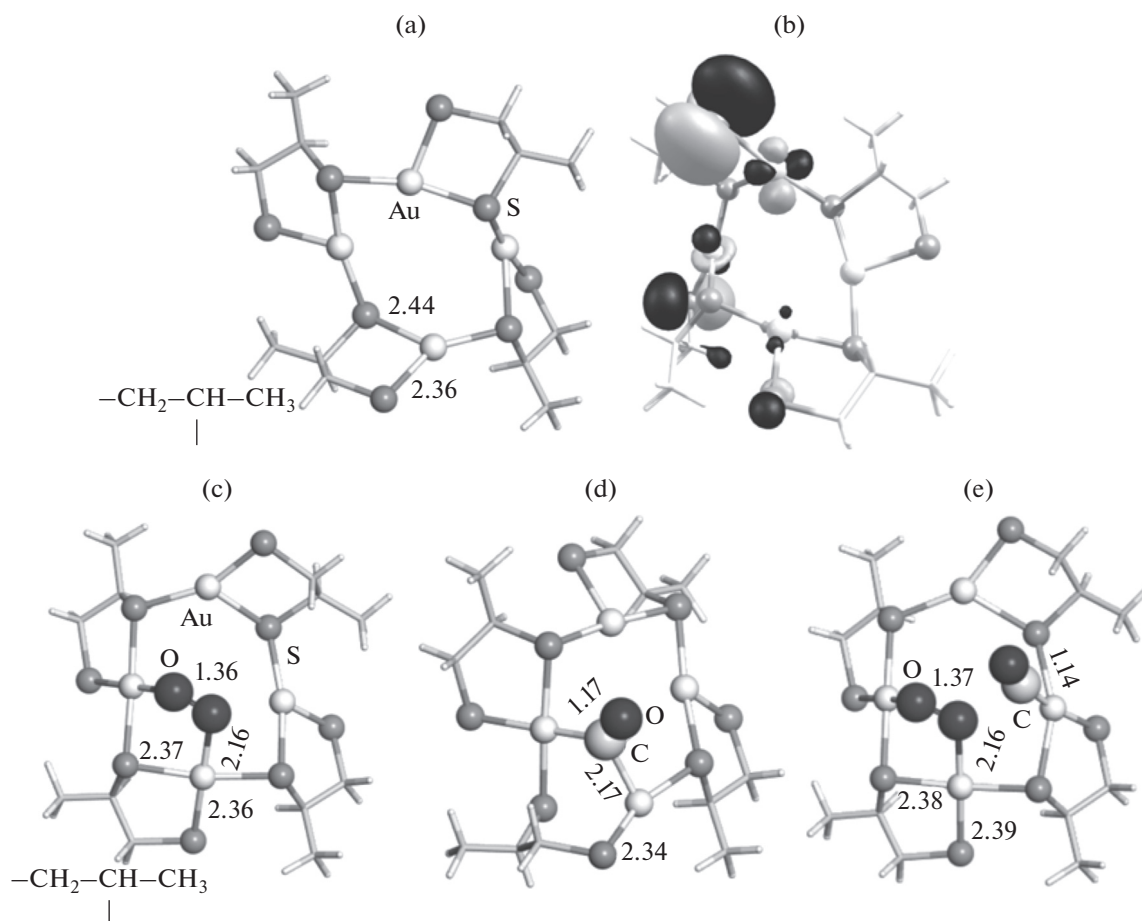
Fig. 2. Optimized structures of the complexes (a) $(AuSCH_2CHSCH_3)_4$, (c) $(AuSCH_2CHSCH_3)_4O_2$, (d) $(AuSCH_2CHSCH_3)_4CO$, and (e) $(AuSCH_2CHSCH_3)_4O_2CO$ and (b) visualization of the HOMO of $(AuSCH_2CHSCH_3)_4$. Key interatomic distances are given in angstrom units.
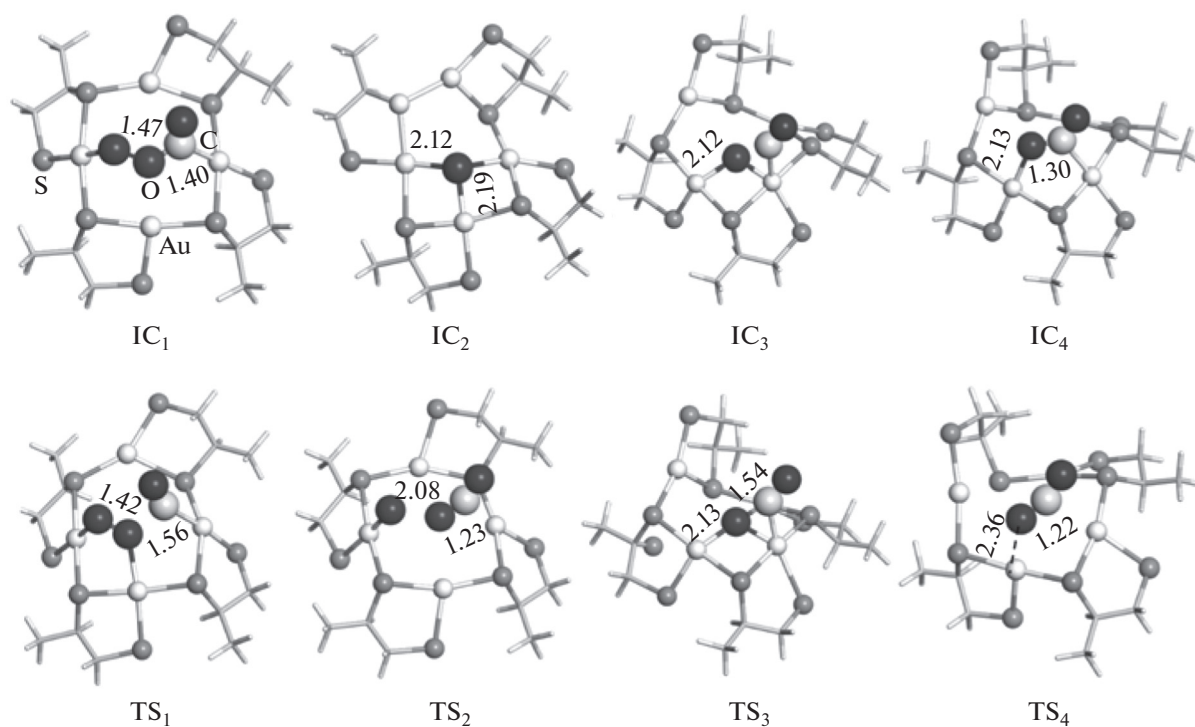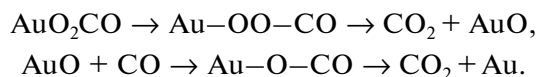
Fig. 3. Optimized structures of the intermediate complexes (ICs) and transition states (TSs) of the steps of CO oxidation from $(AuSCH_2CHSCH_3)_4O_2CO$. Key interatomic distances are given in angstrom units.

A stable peroxo-type complex is formed by the interaction of the dithiolate complex with O_2 (Fig. 2b). In this complex, oxygen is simultaneously bound to two Au atoms. The O–O interatomic distance in $(AuSCH_2CHSCH_3)_4O_2$ increased by 0.07 Å and the O–O vibrational frequency of 921.5 cm^{-1} indicate a significant activation of oxygen. This peroxo complex can be formed from triplet oxygen with an energy gain of −9.1 kcal/mol. The subsequent addition of CO to the oxygen complex is more favorable than the addition of CO to $(AuSCH_2CHSCH_3)_4$. In this case, the effect of co-adsorption is observed as a positive influence of the adsorption of a reactant on the subsequent adsorption of another one. The effect of the co-adsorption of O_2 and CO is well known for the oxidation of CO on gold nanoparticles [37, 38].

As judged from its structure, the found complex $(AuSCH_2CHSCH_3)_4O_2CO$ (IC$_0$) can act as an intermediate (intermediate complex, IC) in the subsequent oxidation of CO. In the simulation of CO_2 formation, we took into account a mechanism known for gold (Au) nanoparticles [39, 40]:

$$AuO_2CO \rightarrow Au–OO–CO \rightarrow CO_2 + AuO,$$
$$AuO + CO \rightarrow Au–O–CO \rightarrow CO_2 + Au.$$

For all steps of this process, we optimized the structure of intermediate complexes (ICs) and transition states (TSs) been (Fig. 3) and calculated the corresponding energies. Figure 4 shows the diagrams of energy changes at the steps of CO oxidation.

The formation of the first molecule of CO_2 occurs in two steps due to low activation energies (Table 2) via
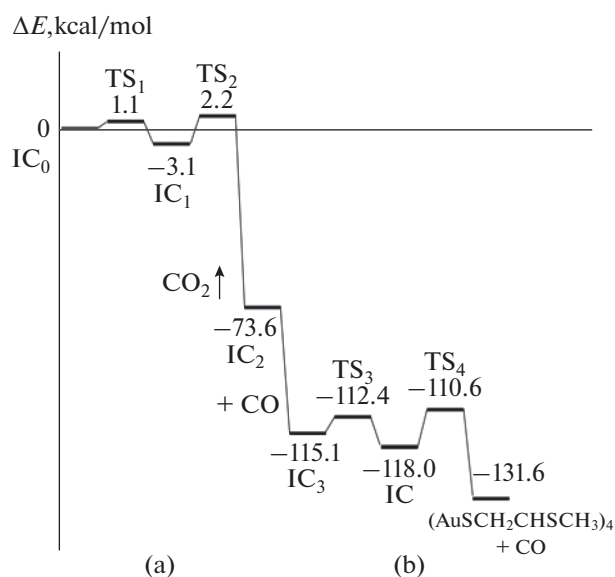

Fig. 4. Energy diagrams of (a) the first two steps of CO oxidation from the initial complex $(AuSCH_2CHSCH_3)4O_2CO$ (IC$_0$) and (b) two steps of the oxidation of the second CO molecule from $(AuSCH_2CHSCH_3)_4OCO$ (IC$_3$).

Table 2. Calculated values of the Gibbs activation energy ($\Delta^{\neq}G_{298}$) and changes in the Gibbs energy (ΔG) for the steps of CO oxidation in the presence of $(AuSCH_2CHSCH_3)_4$

Step	$\Delta^{\neq}G_{298}$	ΔG_{298}
	kcal/mol	
$IC_0 \rightarrow IC_1$	0.9	−0.5
$IC_1 \rightarrow IC_2$	5.2	−81.7
$IC_3 \rightarrow IC_4$	2.3	−0.8
$IC_4 \rightarrow (AuSCH_2CHSCH_3)_4 + CO_2$	6.5	−28.2

the intermediate IC_1. In the intermediate complex IC_2 formed at the final step, the remaining oxygen atom is coordinated to three gold atoms. The second CO molecule is attached at the Au atom bound to O with the formation of the intermediate IC_3. Its conversion into CO_2 and the initial cluster occurs in two steps through the intermediate complex IC_4 with low activation energies.

Thus, according to the calculation data, the complex $(AuSCH_2CHSCH_3)_4$ is more reactive than $(AuSCH_3)_4$ in the activation of O_2 and CO and in the further oxidation of CO. At the steps of the activation of reactants and their transformations, bonds with stabilizing ligands are not ruptured; this is important in the retention of the size and structure of the complex. It is believed that gold clusters stabilized by analogous dithiolate ligands are more promising catalytic systems for CO oxidation than clusters stabilized by thiolate groups. The gold clusters stabilized by dithiolate ligands can be synthesized by ligand exchange, for example, between $Au_{25}(2\text{-}PET)_{18}$ and 1,1'-binaphthyl-2,2'-dithiol (BINAS) [41].

CONCLUSIONS

The structure and reactivity of the cyclic thiolate and dithiolate complexes of Au(I) formed by the −SR−Au−SR−Au− fastening fragment, which is typical of all $Au_n(SR)_m$, were studied for the first time using the density functional theory method. According to the calculation data, the thiolate complex $(AuSCH_3)_4$ is inert with respect to O_2 and CO due to the strong Au−S bond. Upon the replacement of a thiolate ligand by a dithiolate one, the reactivity of the complex toward the test molecules increases considerably. It was shown that $(AuSCH_2CHSCH_3)_4$ or gold clusters containing analogous fragments can act as catalysts for the oxidation of CO. The results are indicative of the important role of a ligand not only in the stabilization of the cluster size or the retention of the complex composition but also in changes in the properties of the complex.

REFERENCES

1. Bond, G.C., Louis, C., and Thompson, D.T., *Catalysis by Gold*, London: Imperial College, 2007.
2. Stratakis, M. and Garcia, H., *Chem. Rev.*, 2012, vol. 112, no. 8, p. 4469.
3. Pichugina, D.A., Kuz'menko, N.E., and Shestakov, A.F., *Russ. Chem. Rev.*, 2015, vol. 84, no. 11, p. 1114.
4. Li, G. and Jin, R., *Acc. Chem. Res.*, 2014, vol. 47, no. 3, p. 816.
5. Zhang, G., Wang, R., and Li, G., *Chin. Chem. Lett.*, 2018, vol. 29, no. 5, p. 687.
6. Akola, J., Walter, M., Whetten, R.L., Häkkinen, H., and Grönbeck, H., *J. Am. Chem. Soc.*, 2008, vol. 130, no. 12, p. 3756.
7. Heaven, M.W., Dass, A., White, P.S., Holt, K.M., and Murray, R.W., *J. Am. Chem. Soc.*, 2008, vol. 130, no. 12, p. 3754.
8. Qian, H., Eckenhoff, W.T., Zhu, Y., Pintauer, T., and Jin, R., *J. Am. Chem. Soc.*, 2010, vol. 132, no. 24, p. 8280.
9. Crasto, D., Malola, S., Brosofsky, G., Dass, A., and Häkkinen, H., *J. Am. Chem. Soc.*, 2014, vol. 136, no. 13, p. 5000.
10. Das, A., Li, T., Li, G., Nobusada, K., Zeng, C., Rosi, N.L., and Jin, R., *Nanoscale*, 2014, vol. 6, p. 6458.
11. Zeng, C., Liu, C., Chen, Y., Rosi, N.L., and Jin, R., *J. Am. Chem. Soc.*, 2014, vol. 136, no. 34, p. 11922.
12. Wang, P., Xiong, L., Sun, X., Ma, Z., and Pei, Y., *Nanoscale*, 2018, vol. 10, no. 8, p. 3918.
13. Yoskamtorn, T., Yamazoe, S., Takahata, R., Nishigaki, J., Thivasasith, A., Limtrakul, J., and Tsukuda, T., *ACS Catal.*, 2014, vol. 4, no. 10, p. 3696.
14. Li, G. and Jin, R., *Nanotechnol. Rev.*, 2013, vol. 2, no. 5, p. 529.

15. Li, G. and Jin, R., *J. Am. Chem. Soc.*, 2014, vol. 136, no. 32, p. 11347.

16. Liu, Y., Tsunoyama, H., Akita, T., Xie, S., and Tsukuda, T., *ACS Catal.*, 2011, vol. 1, no. 1, p. 2.

17. Kurashige, W., Yamaguchi, M., Nobusada, K., and Negishi, Y., *J. Phys. Chem. Lett.*, 2012, vol. 3, no. 18, p. 2649.

18. Harkness, K.M., Cliffel, D.E., and McLean, J.A., *Analyst*, 2010, vol. 135, no. 5, p. 868.

19. Nie, X., Qian, H., Ge, Q., Xu, H., and Jin, R., *ACS Nano*, 2012, vol. 6, p. 6014.

20. Wu, Z., Jiang, D.E., Mann, A.K., Mullins, D.R., Qiao, Z.A., Allard, L.F., Zeng, C., Jin, R., and Overbury, S.H., *J. Am. Chem. Soc.*, 2014, vol. 136, no. 16, p. 6111.

21. Nie, X., Zeng, C., Ma, X., Qian, H., Ge, Q., Xu, H., and Jin, R., *Nanoscale*, 2013, vol. 5, p. 5912.

22. Li, Y., Chen, Y., House, S.D., Zhao, S., Wahab, Z., Yang, J.C., and Jin, R., *ACS Appl. Mater. Interfaces*, 2018, vol. 10, no. 35, p. 29425.

23. Bonasia, P.J., Gindelberger, D.E., and Arnold, J., *Inorg. Chem.*, 1993, vol. 32, no. 23, p. 5126.

24. Perdew, J.P., Burke, K., and Ernzerhof, M., *Phys. Rev. Lett.*, 1996, vol. 77, no. 18, p. 3865.

25. Stevens, W.J., Krauss, M., Basch, H., and Jasien, P.G., *Can. J. Chem.*, 1992, vol. 70, no. 2, p. 612.

26. Nikitina, N.A., Pichugina, D.A., and Kuz'menko, N.E., *Russ. J. Phys. Chem. A*, 2017, vol. 91, no. 8, p. 1507.

27. Pichugina, D.A., Shestakov, A.F., and Kuz'menko, N.E., *Kinet. Catal.*, 2007, vol. 48, no. 2, p. 305.

28. Askerka, M., Pichugina, D., Kuz'menko, N., and Shestakov, A., *J. Phys. Chem. A*, 2012, vol. 116, no. 29, p. 7686.

29. Pichugina, D.A., Nikolaev, S.A., Mukhamedzyanova, D.F., and Kuz'menko, N.E., *Russ. J. Phys. Chem. A*, 2014, vol. 88, no. 6, p. 959.

30. Polynskaya, Y.G., Pichugina, D.A., and Kuz'menko, N.E., *Comput. Theor. Chem.*, 2015, vol. 1055, p. 61.

31. Schlegel, H.B., *J. Comput. Chem.*, 1982, vol. 3, no. 2, p. 214.

32. Gonzalez, C., and Schlegel, H.B., *J. Chem. Phys.*, 1989, vol. 90, no. 4, p. 2154.

33. Laikov, D.N. and Ustynyuk, Yu.A., *Russ. Chem. Bull.*, 2005, no. 3, p. 820.

34. Sadovnichy, V., Tikhonravov, A., Voevodin, Vl., and Opanasenko, V., *Contemporary High Performance Computing: From Petascale toward Exascale*, Boca Raton: CRC Press, 2013, p. 283.

35. Kawasaki, H., Kumar, S., Li, G., Zeng, C., Kauffman, D.R., Yoshimoto, J., Iwasaki, Y., and Jin, R., *Chem. Mater.*, 2014, vol. 26, no. 9, p. 2777.

36. Li, Z., Liu, C., Abroshan, H., Kauffman, D.R., and Li, G., *ACS Catal.*, 2017, vol. 7, no. 5, p. 3368.

37. Li, L., Gao, Y., Li, H., Zhao, Y., Pei, Y., Chen, Z., and Zeng, X.C., *J. Am. Chem. Soc.*, 2013, vol. 135, no. 51, p. 19336.

38. Zeng, W., Tang, J., Wanga, P., and Pei, Y., *RSC Adv.*, 2016, vol. 6, p. 55867.

39. Haruta, M., *Gold Bull.*, 2004, vol. 37, p. 27.

40. Bond, G.C. and Thompson, D.T., *Gold Bull.*, 2000, vol. 33, p. 41.

41. Knoppew, S. and Bürgi, T., *Phys. Chem. Chem. Phys.*, 2013, vol. 15, p. 15816.

Translated by Valentin Makhlyarchuk

SPELL: 1. OK